Quest Journals
Journal of Electronics and Communication Engineering Research
Volume 12 ~ Issue 4 (Jul. – Aug. 2026) pp: 33-41
ISSN(Online): 2321-5941
www.questjournals.org

Research Paper

Optimization of Adaptive Smart Antenna Systems for Enhanced Signal Quality and Interference Management

Surendra Prasad
Research Scholar, University Department of Physics,
Munger University, Munger

Ansu Kumar Roy
Supervisor, Assistant Professor, University Department of Physics,
Munger University, Munger

Abstract
Adaptive smart antennas improve wireless-link performance by adjusting the complex excitation weights of individual antenna elements according to the spatial characteristics of the received signals. Their practical effectiveness, however, depends strongly on algorithmic parameters, covariance estimation, convergence rate, steering-vector accuracy, and computational complexity. This study develops and evaluates a parameter-optimization framework for adaptive smart antenna systems using normalized least mean square, recursive least square, sample-matrix-inversion minimum variance distortionless response, and diagonally loaded minimum variance distortionless response beamformers. An eight-element half-wavelength uniform linear array was simulated in a co-channel interference environment containing a quadrature phase-shift keyed desired signal and two strong interferers. Steering-direction uncertainty, element-gain variation, and phase mismatch were incorporated into the data model. Algorithmic parameters were selected using 60 independent validation realizations and evaluated using 300 independent Monte Carlo realizations. Each evaluation contained 500 adaptation symbols and 2,000 test symbols. The optimized recursive least square beamformer produced the highest mean output signal-to-interference-plus-noise ratio of 8.705 dB and the lowest bit-error rate of 0.00328. Relative to unregularized sample-matrix-inversion beamforming, it generated a 4.780 dB SINR gain, approximately tripled the linear SINR, and reduced bit-error rate by 95.51%. Repeated-measures analysis indicated a statistically significant algorithm effect, ($F(4, 1196) = 5220.06$), ($p < 0.001$), with partial ($\eta^2 = 0.946$). The findings demonstrate that adaptive-parameter tuning and covariance regularization are essential for obtaining stable signal enhancement and interference suppression under practical array mismatch.

Keywords: *adaptive beamforming, smart antenna, interference suppression, MVDR, diagonal loading, NLMS, RLS, signal-to-interference-plus-noise ratio.*

I. Introduction

The increasing density of wireless devices, frequency reuse, multipath propagation, and spectrum sharing has made co-channel interference a principal limitation on communication reliability. Increasing transmitter power alone cannot adequately address this limitation because it may strengthen interference in neighbouring links and increase energy consumption. Smart antenna systems provide a spatial-domain solution by combining signals received through multiple antenna elements with adaptively controlled complex weights. These weights reinforce signals arriving from the desired direction while attenuating signals originating from interfering directions.

The foundations of adaptive antenna processing were established by Widrow *et al.*, who demonstrated that least-mean-square adaptation could automatically modify array weights to suppress directional interference [1]. The minimum-variance formulation introduced by Capon subsequently provided a method for minimizing array output power while preserving a distortionless response in a selected direction [2]. Frost extended constrained adaptation by maintaining a prescribed response toward the signal of interest while minimizing interference and noise power [3]. These developments established the principal mathematical structure used in contemporary adaptive beamforming.

Adaptive beamforming algorithms nevertheless exhibit substantially different convergence and robustness characteristics. Gradient-based algorithms have comparatively low computational requirements but may converge slowly when the received-signal covariance matrix has a large eigenvalue spread. Sample-matrix and recursive techniques converge more rapidly, although they require greater computational resources and may become sensitive to covariance-estimation error. Reed, Mallett, and Brennan showed that the number of available training snapshots is central to adaptive-array performance because limited covariance observations produce substantial signal-to-noise-ratio loss [4].

Minimum variance distortionless response (MVDR) beamforming is theoretically attractive when the covariance matrix and steering vector are accurately known. In practical systems, however, array calibration errors, local scattering, direction-of-arrival estimation errors, mutual coupling, and finite sample sizes produce steering-vector mismatch. Under such conditions, an unregularized MVDR beamformer may partially suppress the desired signal. Worst-case optimization and robust Capon beamforming were developed to reduce this vulnerability by accounting for uncertainty in the assumed steering vector [5], [6]. Diagonal loading is particularly useful because it improves covariance conditioning while reducing excessive adaptation to sample-specific interference structure.

The importance of implementation-aware optimization has increased with digital and hybrid beamforming systems. Software-defined-radio experiments have demonstrated that LMS, recursive least square (RLS), sample-matrix-inversion (SMI), and MVDR-type techniques can suppress strong interference, while also showing that synchronization, calibration, carrier offset, and multipath conditions materially affect practical performance [7]. Hybrid beamforming prototypes and multi-cell systems further indicate that antenna-array optimization must balance spatial selectivity, radio-frequency-chain requirements, processing overhead, and interference coordination [8], [9].

Recent research has expanded adaptive beamforming toward low-complexity beam tracking, sparse array reconfiguration, and learning-assisted coordination. LMS-based beam tracking can remain effective under imperfect angular initialization, while regularized antenna-selection methods can jointly optimize array configuration and excitation weights [10], [11]. Deep reinforcement learning has also been applied to joint beamforming, power control, and interference coordination, illustrating the movement toward environment-aware optimization [12].

Despite these advances, many comparative studies employ fixed step sizes, forgetting factors, or loading parameters. Such comparisons may reflect arbitrary parameter selection rather than the intrinsic suitability of an algorithm. The present study therefore optimizes the principal control parameters of NLMS, RLS, and diagonally loaded MVDR beamformers under identical array and interference conditions. The specific objectives are:

1. to formulate a realistic adaptive smart antenna model incorporating co-channel interference, angular uncertainty, and element calibration errors;
2. to determine optimal NLMS step size, RLS forgetting factor, and MVDR diagonal-loading level;
3. to compare optimized algorithms using output SINR, bit-error rate, convergence speed, and computational order; and
4. to statistically test whether observed performance differences remain significant across independent channel realizations.

II. Signal Model and Beamforming Formulation

Array signal model

An (M)-element uniform linear array with inter-element spacing ($d = \lambda_c/2$) was considered, where (λ_c) denotes carrier wavelength. The complex steering vector corresponding to an incident signal from angle (θ) is

$$\mathbf{a}(\theta) = \begin{bmatrix}1 & e^{j\pi \sin\theta} & \cdots & e^{j\pi(M-1)\sin\theta}\end{bmatrix}^T .$$

For one desired signal and (K) interfering signals, the received array snapshot is

$$\mathbf{x}(n) = \mathbf{a}s s(n) + \sum k = 1^K \mathbf{a}_k i_k(n) + \mathbf{v}(n),$$

where ($s(n)$) is the desired symbol, ($i_k(n)$) is the (k)-th interference symbol, and ($\mathbf{v}(n)$) is spatially white complex Gaussian noise.

The beamformer output is

$$y(n) = \mathbf{w}^H \mathbf{x}(n),$$

where (\mathbf{w}) is the complex weight vector and (H) denotes the Hermitian transpose. The output SINR is

$$\mathrm{SINRout} = \frac{P_s \left|\mathbf{w}^H \mathbf{a}s\right|^2}{} \sum_{k=1}^{K} P_{i_k} \left|\mathbf{w}^H \mathbf{a}_k\right|^2 + \sigma_v^2 \mathbf{w}^H \mathbf{w}.$$

This expression simultaneously measures desired-signal preservation, spatial interference rejection, and noise amplification.

Conventional beamformer
The conventional delay-and-sum beamformer was used as the non-adaptive baseline:

$$\mathbf{w}_{\mathrm{CBF}} = \frac{\mathbf{a}_0}{\mathbf{a}_0^H \mathbf{a}_0},$$

where ($\mathbf{a}_0$) is the steering vector calculated from the nominal desired direction. It provides coherent array gain but does not explicitly place nulls toward interference sources.

Normalized least mean square beamformer
The NLMS update was defined as

$$e(n) = d(n) - \mathbf{w}^H(n)\mathbf{x}(n),$$
$$\mathbf{w}(n+1) = \mathbf{w}(n) + \frac{\mu}{\epsilon + \mathbf{x}^H(n)\mathbf{x}(n)}\mathbf{x}(n)e^*(n),$$

where ($d(n)$) is the desired training symbol, (μ) is the normalized step size, and (ϵ) prevents division by a small value. Normalization limits the effect of rapid changes in received power, although convergence and residual misadjustment remain dependent on (μ). The trade-off between low-complexity stochastic-gradient adaptation and convergence speed is consistent with classical and contemporary constrained beamforming research [1], [10].

Recursive least square beamformer
The RLS algorithm recursively minimizes an exponentially weighted squared-error criterion:

$$J(n) = \sum_{\ell=1}^{n} \lambda^{n-\ell} \left| d(\ell) - \mathbf{w}^H(n)\mathbf{x}(\ell) \right|^2,$$

where (λ) is the forgetting factor. The gain and weight updates are

$$\mathbf{k}(n) = \frac{\mathbf{P}(n-1)\mathbf{x}(n)}{\lambda + \mathbf{x}^H(n)\mathbf{P}(n-1)\mathbf{x}(n)},$$
$$\mathbf{w}(n) = \mathbf{w}(n-1) + \mathbf{k}(n)e^*(n),$$
$$\mathbf{P}(n) = \lambda^{-1}\left[\mathbf{P}(n-1) - \mathbf{k}(n)\mathbf{x}^H(n)\mathbf{P}(n-1)\right].$$

RLS usually converges faster than stochastic-gradient adaptation but requires approximately ($O(M^2)$) operations per update. Research on constrained and set-membership beamforming similarly reports that RLS-type methods offer rapid convergence at the cost of higher computational requirements and possible numerical sensitivity [4], [13].

MVDR and diagonal loading
The sample covariance matrix was estimated as

$$\widehat{\mathbf{R}} = \frac{1}{N}\sum_{n=1}^{N} \mathbf{x}(n)\mathbf{x}^H(n).$$

The SMI-MVDR weight vector was

$$\mathbf{w}_{\mathrm{MVDR}} = \frac{\widehat{\mathbf{R}}^{-1}\mathbf{a}_0}{\mathbf{a}_0^H \widehat{\mathbf{R}}^{-1}\mathbf{a}_0}.$$

For the diagonally loaded MVDR beamformer,

$$\widehat{\mathbf{R}}_{\mathrm{DL}} = \widehat{\mathbf{R}} + \alpha \frac{\mathrm{tr}(\widehat{\mathbf{R}})}{M}\mathbf{I},$$

where (α) is the normalized loading coefficient. The optimized weight vector becomes

$$\mathbf{w}\mathrm{DL} = \frac{\widehat{\mathbf{R}}\mathrm{DL}^{-1}\mathbf{a}_0}{\mathbf{a}0^H \widehat{\mathbf{R}}\mathrm{DL}^{-1}\mathbf{a}_0}.$$

Diagonal loading improves numerical conditioning and reduces sensitivity to covariance and steering-vector errors, although excessive loading causes the solution to approach conventional beamforming [6].

III. Methodology

The numerical experiment used an eight-element uniform linear array. The nominal desired-signal direction was (10°), while two interfering signals arrived from approximately (-25°) and (35°). QPSK modulation was used for the desired and interfering signals.

To prevent the analysis from representing an idealized perfectly calibrated array, the actual desired direction in each realization was drawn from a normal distribution with mean (10°) and standard deviation (1.5°). Interference directions included a standard deviation of (0.6°). Independent element-gain errors with a standard deviation of 3% and element-phase errors with a standard deviation of (2°) were also applied.

Table 1. Simulation parameters

Parameter	Value
Number of antenna elements (M)	8
Element spacing	($0.5\lambda_c$)
Nominal desired direction	(10°)
Interference directions	(-25°), (35°)
Input SNR in principal experiment	0 dB
Interference-to-noise ratios	20 dB and 15 dB
Modulation	QPSK
Adaptation symbols per realization	500
Independent test symbols	2,000
Validation realizations	60
Evaluation realizations	300
Desired-angle uncertainty	($N(0, 1.5^2)$) degrees
Element-gain standard deviation	3%
Element-phase standard deviation	(2°)

Each algorithm was trained using the same received snapshots within a realization. Performance was then measured on an independent block of 2,000 symbols, preventing the reported bit-error rate from being calculated on the adaptation data.

The optimization stage used 60 independent validation realizations. Mean output SINR was the optimization criterion. The following parameter grids were examined:

$$\mu \in 0.02, 0.05, 0.10, 0.20, 0.40, 0.70, 1.00,$$
$$\lambda \in 0.94, 0.96, 0.98, 0.99, 0.995, 0.999,$$

And

$$\alpha \in 0, 10^{-4}, 3 \times 10^{-4}, 10^{-3}, 3 \times 10^{-3}, 10^{-2}, 3 \times 10^{-2}, 0.1, 0.3, 1.0.$$

The best-performing values were ($\mu = 0.05$), ($\lambda = 0.999$), and ($\alpha = 0.10$).

Table 2. Optimized parameters and validation performance

Algorithm	Selected parameter	Mean validation SINR (dB)
NLMS	($\mu = 0.05$)	8.482
RLS	($\lambda = 0.999$)	8.728
DL-MVDR	($\alpha = 0.10$)	8.246

The NLMS results displayed the expected adaptation trade-off. Increasing (\mu) beyond 0.05 accelerated early weight changes but increased steady-state fluctuation. The RLS result favoured a forgetting factor close to unity because the principal experiment was approximately stationary over the 500-symbol training block. The loading search produced a unimodal pattern: small values did not sufficiently regularize the covariance matrix, whereas large values weakened adaptive interference rejection.

Performance and statistical analysis

The principal performance measures were output SINR, uncoded QPSK bit-error rate, and convergence speed. Convergence was defined as the first snapshot at which the 20-snapshot smoothed mean output SINR remained within 1 dB of its final steady-state value.

Because every algorithm was evaluated on the same 300 realizations, algorithm performance constituted a repeated-measures design. A repeated-measures analysis of variance was applied to SINR values. The Friedman test was additionally used as a distribution-free verification. Pairwise dependent-sample comparisons were adjusted by the Holm procedure. Effect size was reported using partial eta squared for the overall analysis and standardized paired difference (d_z) for selected comparisons.

IV. Results

Output SINR and bit-error rate

Table 3. Principal performance results over 300 realizations

Algorithm	Mean output SINR (dB)	SD (dB)	95% CI of mean (dB)	Mean BER
Conventional beamformer	-5.576	0.594	-5.644 to -5.509	0.29597
SMI-MVDR	3.925	3.404	3.538 to 4.312	0.07311
Optimized NLMS	8.416	0.373	8.374 to 8.458	0.00446
Optimized RLS	**8.705**	**0.118**	**8.692 to 8.718**	**0.00328**
Optimized DL-MVDR	8.140	0.534	8.079 to 8.200	0.00588

The conventional beamformer exhibited a negative mean output SINR because it provided array gain toward the desired direction without actively suppressing the two high-power interferers. SMI-MVDR improved the mean SINR by 9.501 dB over conventional beamforming, but its standard deviation of 3.404 dB indicated considerable sensitivity to steering mismatch.

Optimized NLMS, RLS, and DL-MVDR all exceeded 8 dB mean output SINR. The optimized RLS beamformer achieved the best result, exceeding unregularized SMI-MVDR by 4.780 dB. This difference corresponds to a linear SINR factor of approximately 3.01. Its bit-error rate declined from 0.07311 for SMI-MVDR to 0.00328, representing a relative reduction of 95.51%.

The small RLS standard deviation indicates that its reference-assisted adaptation consistently separated the desired training sequence from interference despite angular and element mismatch. DL-MVDR also performed reliably, but it retained dependence on the nominal steering vector. NLMS approached the RLS steady-state result with much lower computational complexity.

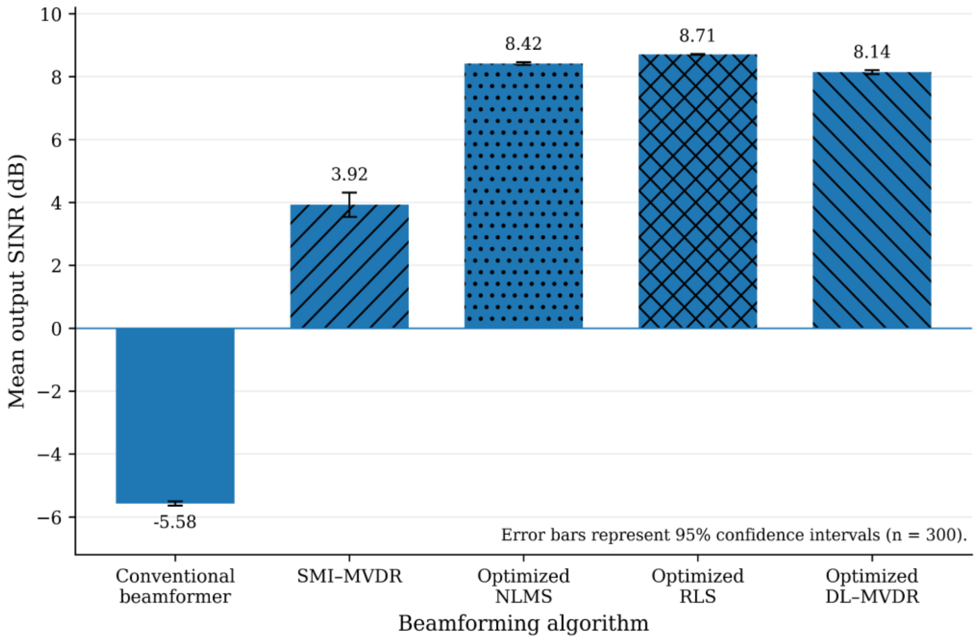

Figure 1. Mean output SINR by beamforming algorithm.

Statistical significance

The repeated-measures analysis demonstrated a significant algorithm effect:

$$F(4, 1196) = 5220.06, \qquad p < 0.001,$$

With

$$\eta_p^2 = 0.946.$$

Thus, approximately 94.6% of the within-realization variance in output SINR was associated with beamforming method. The Friedman test confirmed the result:

$$\chi_F^2(4) = 1150.79, \qquad p < 0.001.$$

The optimized RLS beamformer exceeded optimized NLMS by 0.289 dB:

$$t(299) = 13.49, \qquad p_{\text{Holm}} < 0.001,$$

$$d_z = 0.779.$$

It exceeded optimized DL-MVDR by 0.566 dB:

$$t(299) = 17.93, \qquad p_{\text{Holm}} < 0.001,$$

$$d_z = 1.035.$$

Optimized NLMS also outperformed DL-MVDR by 0.276 dB:

$$t(299) = 17.41, \qquad p_{\text{Holm}} < 0.001.$$

Although the numerical difference between RLS and NLMS was below 0.3 dB, its consistency across independent realizations generated a statistically strong effect. Practical selection should therefore consider whether this additional gain justifies the quadratic computational cost of RLS.

Convergence performance

Table 4. Average learning-curve values

Adaptation snapshot	Optimized NLMS SINR (dB)	Optimized RLS SINR (dB)
10	-3.497	5.115
25	-0.948	7.346
50	2.085	8.088
100	5.565	8.402
200	8.068	8.585
500	8.414	8.686

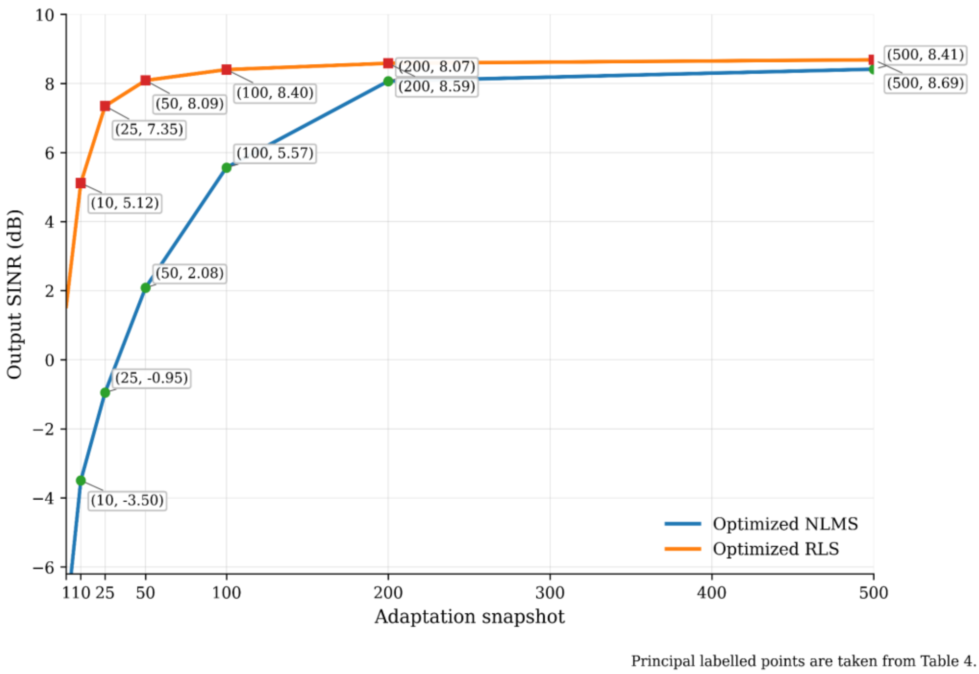

Figure 2. Convergence of optimized NLMS and RLS beamformers.

RLS entered the 1-dB steady-state region after approximately 44 snapshots, whereas NLMS required approximately 162 snapshots. Therefore, RLS convergence was about 3.7 times faster under the adopted criterion. Its rapid convergence is important in packet-based systems where only a limited preamble or pilot sequence is available. The NLMS result remains valuable for continuously operating systems in which lower processing cost and numerical simplicity are more important than initial adaptation speed.

Sensitivity to input SNR

Table 5. Mean output SINR under different input-SNR conditions

Algorithm	-5 dB input SNR	0 dB	5 dB	10 dB
Conventional	-10.505	-5.536	-0.558	4.381
SMI-MVDR	2.010	4.030	2.497	-0.671
Optimized NLMS	3.436	8.498	13.416	18.487
Optimized RLS	**3.679**	**8.721**	**13.722**	**18.693**
Optimized DL-MVDR	3.333	8.207	12.395	15.288

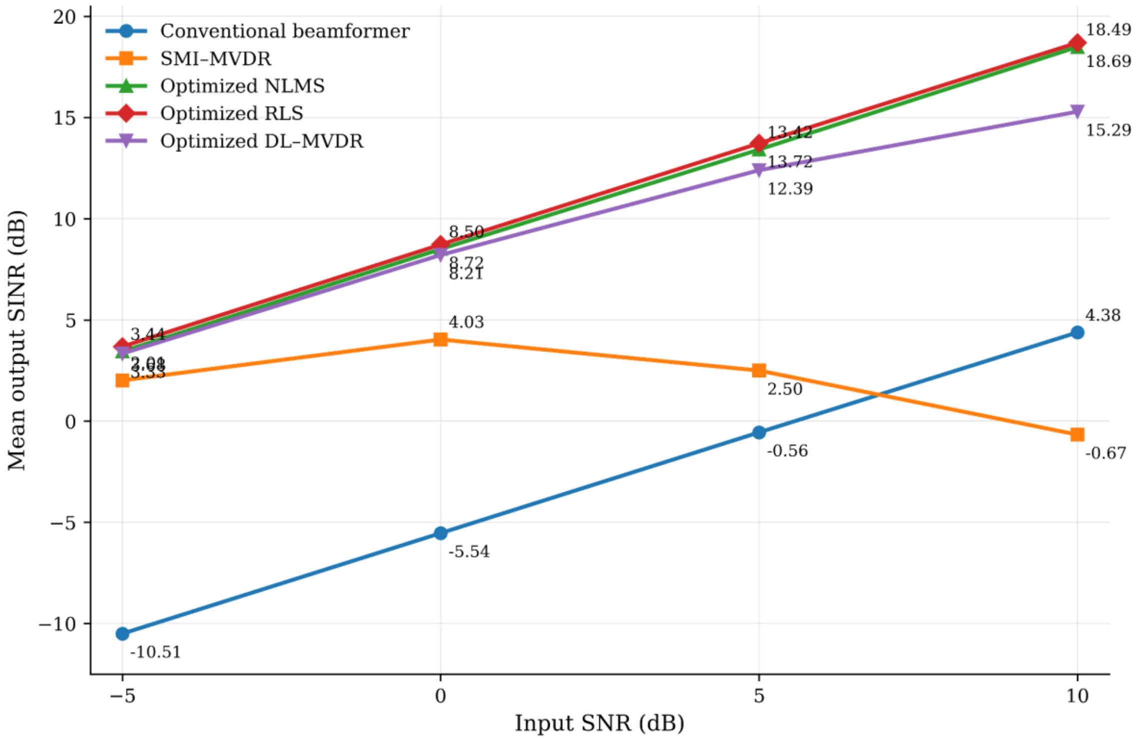

Figure 3. Output SINR versus input SNR.

The optimized adaptive algorithms improved as input SNR increased. In contrast, SMI-MVDR deteriorated at high input SNR. This result is not contradictory: when the desired signal becomes strong and its actual steering vector differs from the assumed vector, the desired-signal component contaminates the covariance estimate. The unregularized minimum-variance solution may then treat part of the desired signal as output power to be minimized. This self-nulling phenomenon is a central reason for robust Capon and worst-case beamforming methods [5], [6].

Diagonal loading reduced this failure but did not completely eliminate mismatch sensitivity. RLS remained strongest because its training reference identified the desired waveform independently of the nominal steering vector.

Computational considerations

For an (M)-element array, conventional beamforming and NLMS require approximately ($O(M)$) operations per snapshot. RLS requires ($O(M^2)$) operations because it updates an inverse-correlation matrix.

SMI-MVDR and DL-MVDR require covariance formation followed by an ($M \times M$) linear-system solution, conventionally associated with ($O(M^3)$) batch complexity.

For the eight-element array, all algorithms were numerically manageable. Nevertheless, the distinction becomes important in massive-array or embedded implementations. Data-selective updates, reduced-rank processing, conjugate-gradient methods, and sparse antenna switching can reduce computation without entirely sacrificing adaptive performance [11], [13].

V. Discussion

The study demonstrates that adaptive smart antenna performance cannot be evaluated independently of parameter optimization. An NLMS beamformer with an excessively large step size may appear inferior because of steady-state misadjustment, while an overly small step size may not converge within the available training interval. Similarly, an RLS forgetting factor selected without reference to channel stationarity can either suppress useful historical information or prevent timely tracking. The loading factor of a robust MVDR beamformer directly determines the balance between adaptive null formation and steering-vector tolerance.

Among the evaluated algorithms, RLS provided the best combination of steady-state SINR, BER, robustness, and convergence speed. Its effectiveness resulted from reference-assisted minimization rather than exclusive dependence on a nominal array manifold. It is therefore especially suitable for systems containing known pilots, preambles, or training sequences. However, its ($O(M^2)$) update complexity and matrix-recursion requirements must be considered in large arrays and low-power receivers.

Optimized NLMS achieved output SINR within 0.289 dB of RLS while requiring substantially lower computational effort. This makes NLMS attractive for mobile terminals, internet-of-things gateways, and software-defined-radio platforms with moderate mobility and adequate adaptation time. Its principal limitation was slower convergence, which may reduce performance when the interference geometry changes rapidly.

The DL-MVDR beamformer offered a useful compromise where no desired waveform reference is available. It substantially outperformed unregularized SMI-MVDR and maintained low BER under moderate steering uncertainty. Its performance confirms that covariance regularization should not be treated as an optional numerical adjustment. Rather, diagonal loading functions as a robustness mechanism that limits excessive reliance on an uncertain covariance estimate and nominal steering vector.

The poor high-SNR performance of unregularized SMI-MVDR is particularly important. Increasing desired-signal power does not guarantee improved adaptive-array output when the presumed and actual steering vectors differ. At high SNR, steering mismatch can become more damaging because the covariance matrix contains a stronger desired-signal component. The beamformer may consequently form an unintended notch near the actual desired direction. Robust optimization, calibration, training-assisted adaptation, or steering-vector estimation is therefore necessary.

Implementation studies using SDR arrays have similarly shown that calibration, synchronization, carrier-frequency offset, and multipath diversity influence measured adaptive-nulling performance [7]. The present simulation extends this principle by quantifying how angular uncertainty and element mismatch interact with algorithm selection and parameter tuning.

The results also have implications for future hybrid and learning-assisted arrays. Joint optimization of beam direction, transmit power, interference coordination, array sparsity, and RF-chain allocation creates a high-dimensional design problem. Learning-based approaches may accelerate online decisions, but classical adaptive filters remain valuable because they are interpretable, require limited training data, and provide predictable convergence behaviour. Deep reinforcement learning and adaptive sparse-array research should therefore be viewed as extensions of, rather than complete replacements for, covariance-based and error-driven beamforming [11], [12].

VI. Conclusion

This study developed a reproducible optimization and evaluation framework for adaptive smart antenna systems operating under strong co-channel interference and realistic array mismatch. NLMS step size, RLS forgetting factor, and MVDR diagonal loading were optimized on independent validation data before final evaluation.

The optimized RLS beamformer achieved the highest output SINR of 8.705 dB, the lowest BER of 0.00328, and convergence within approximately 44 snapshots. Optimized NLMS attained 8.416 dB output SINR with lower computational complexity but required approximately 162 snapshots to approach steady-state performance. Optimized DL-MVDR produced 8.140 dB and provided a robust reference-free alternative. Unregularized SMI-MVDR was highly variable and became vulnerable to desired-signal cancellation as input SNR and steering mismatch increased.

The statistical analysis confirmed that algorithm selection produced a substantial effect on signal quality. The central engineering conclusion is that adaptive smart antennas should be designed through joint consideration of convergence, covariance conditioning, steering uncertainty, training availability, and computational resources. Parameter-optimized RLS is preferable when rapid convergence and training references are available; NLMS is suitable for low-complexity continuous adaptation; and diagonally loaded MVDR is appropriate when reference-free operation and mismatch robustness are required.

References

[1]. B. Widrow, P. E. Mantey, L. J. Griffiths, and B. B. Goode, "Adaptive antenna systems," *Proceedings of the IEEE*, vol. 55, no. 12, pp. 2143–2159, Dec. 1967.

[2]. J. Capon, "High-resolution frequency-wavenumber spectrum analysis," *Proceedings of the IEEE*, vol. 57, no. 8, pp. 1408–1418, Aug. 1969.

[3]. O. L. Frost III, "An algorithm for linearly constrained adaptive array processing," *Proceedings of the IEEE*, vol. 60, no. 8, pp. 926–935, Aug. 1972.

[4]. I. S. Reed, J. D. Mallett, and L. E. Brennan, "Rapid convergence rate in adaptive arrays," *IEEE Transactions on Aerospace and Electronic Systems*, vol. AES-10, no. 6, pp. 853–863, Nov. 1974.

[5]. S. A. Vorobyov, A. B. Gershman, and Z.-Q. Luo, "Robust adaptive beamforming using worst-case performance optimization: A solution to the signal mismatch problem," *IEEE Transactions on Signal Processing*, vol. 51, no. 2, pp. 313–324, Feb. 2003.

[6]. J. Li, P. Stoica, and Z. Wang, "On robust Capon beamforming and diagonal loading," *IEEE Transactions on Signal Processing*, vol. 51, no. 7, pp. 1702–1715, Jul. 2003.

[7]. D. C. Gaydos, P. Nayeri, and R. L. Haupt, "Adaptive beamforming with software-defined-radio arrays," *IEEE Access*, vol. 10, pp. 11669–11678, 2022.

[8]. J. Jang *et al.*, "Smart small cell with hybrid beamforming for 5G: Theoretical feasibility and prototype results," *IEEE Wireless Communications*, vol. 23, no. 6, pp. 124–131, Dec. 2016.

[9]. S. Sun, T. S. Rappaport, and M. Shafi, "Hybrid beamforming for 5G millimeter-wave multi-cell networks," in *Proc. IEEE INFOCOM Workshops*, Honolulu, HI, USA, 2018, pp. 589–596.

[10]. Y. Yapici and I. Guvenc, "Low-complexity adaptive beam and channel tracking for mobile mmWave communications," in *Proc. 52nd Asilomar Conf. Signals, Systems, and Computers*, Pacific Grove, CA, USA, 2018, pp. 572–576.

[11]. X. Wang, M. S. Greco, and F. Gini, "Adaptive sparse array beamformer design by regularized complementary antenna switching," *IEEE Transactions on Signal Processing*, vol. 69, pp. 2302–2315, 2021.

[12]. F. B. Mismar, B. L. Evans, and A. Alkhateeb, "Deep reinforcement learning for 5G networks: Joint beamforming, power control, and interference coordination," *IEEE Transactions on Communications*, vol. 68, no. 3, pp. 1581–1592, Mar. 2020.

[13]. L. Wang and R. C. de Lamare, "Set-membership constrained conjugate gradient beamforming algorithms," arXiv:1302.0422, 2013.